Environmental Microbiology (2006) **8**(12), 2214–2223 doi:10.1111/j.1462-2920.2006.01160.x

Fungal hydroquinones contribute to brown rot of wood

Melissa R. Suzuki,[1] Christopher G. Hunt,[1] Carl J. Houtman,[1] Zachary D. Dalebroux[2] and Kenneth E. Hammel[1,2]*

[1]*USDA Forest Products Laboratory, Madison, WI 53726, USA.*

[2]*Department of Bacteriology, University of Wisconsin, Madison, WI 53706, USA.*

Summary

The fungi that cause brown rot of wood initiate lignocellulose breakdown with an extracellular Fenton system in which Fe^{2+} and H_2O_2 react to produce hydroxyl radicals (•OH), which then oxidize and cleave the wood holocellulose. One such fungus, *Gloeophyllum trabeum*, drives Fenton chemistry on defined media by reducing Fe^{3+} and O_2 with two extracellular hydroquinones, 2,5-dimethoxyhydroquinone (2,5-DMHQ) and 4,5-dimethoxycatechol (4,5-DMC). However, it has never been shown that the hydroquinones contribute to brown rot of wood. We grew *G. trabeum* on spruce blocks and found that 2,5-DMHQ and 4,5-DMC were each present in the aqueous phase at concentrations near 20 μM after 1 week. We determined rate constants for the reactions of 2,5-DMHQ and 4,5-DMC with the Fe^{3+}-oxalate complexes that predominate in wood undergoing brown rot, finding them to be 43 l mol^{-1} s^{-1} and 65 l mol^{-1} s^{-1} respectively. Using these values, we estimated that the average amount of hydroquinone-driven •OH production during the first week of decay was 11.5 μmol g^{-1} dry weight of wood. Viscometry of the degraded wood holocellulose coupled with computer modelling showed that a number of the same general magnitude, 41.2 μmol oxidations per gram, was required to account for the depolymerization that occurred in the first week. Moreover, the decrease in holocellulose viscosity was correlated with the measured concentrations of hydroquinones. Therefore, hydroquinone-driven Fenton chemistry is one component of the biodegradative arsenal that *G. trabeum* expresses on wood.

Received 14 July, 2006; accepted 13 September, 2006. *For correspondence. E-mail kehammel@wisc.edu; Tel. (+1) 608 231 9528; Fax (+1) 608 231 9262.

Introduction

Most terrestrial carbon is sequestered in lignocellulose or soil derived from it, and the flux through these pools has a large effect on global carbon balance. Boreal forests that are dominated by conifers contain a disproportionate share of this fixed carbon, because their low temperatures and nutrient-poor soils impede lignocellulose breakdown. Roughly one quarter of global soil carbon is thought to reside in boreal forests, and much of this consists of woody debris undergoing decay by brown rot basidiomycetes (McFee and Stone, 1966; Lindahl *et al*., 2002). These important fungi attack wood by first depolymerizing its holocellulose, even though no known cellulase or hemicellulase is small enough to penetrate the lignified cell wall at the outset of decay (Cowling, 1961; Flournoy *et al*., 1991). The chemical changes that occur in the cellulose during decay, and the sensitivity of biodegradation to antioxidants, indicate that the depolymerizing agent is not a polysaccharidase, but rather a highly reactive, non-selective oxidant (Kirk *et al*., 1991; Schultz and Nicholas, 2002). The hydroxyl radical, which is generally produced in biological systems via Fenton chemistry ($H_2O_2 + Fe^{2+} + H^+ \rightarrow H_2O + Fe^{3+} + \bullet OH$), has long been considered the most likely candidate (Koenigs, 1974; Illman *et al*., 1989; Hammel *et al*., 2002). Experiments with brown rot fungi grown on defined media indicate, in agreement with this hypothesis, that they employ •OH to initiate the biodegradation of many synthetic polymers and organopollutants (Wetzstein *et al*., 1997; Kerem *et al*., 1998; Schlosser *et al*., 2000; Cohen *et al*., 2002; Newcombe *et al*., 2002; Kramer *et al*., 2004).

For the Fenton reaction to occur outside the fungal hyphae, an extracellular mechanism must exist to produce Fe^{2+} and H_2O_2. The brown rot fungus *Gloeophyllum trabeum* does this on defined media by secreting two hydroquinones, 2,5-dimethoxyhydroquinone (2,5-DMHQ) and 4,5-dimethoxycatechol (4,5-DMC), that reduce Fe^{3+} to give Fe^{2+} and semiquinone radicals (Kerem *et al*., 1999; Paszczynski *et al*., 1999; Jensen *et al*., 2001; Newcombe *et al*., 2002). The semiquinones reduce both O_2 and Fe^{3+}, giving perhydroxyl radicals (•OOH), additional Fe^{2+} and the two quinones: 2,5-dimethoxy-1,4-benzoquinone (2,5-DMBQ) and 4,5-dimethoxy-1,2-benzoquinone (4,5-DMBQ). The simultaneous presence of Fe^{2+} and •OOH initiates oxidoreductions in which the Fe^{2+}/Fe^{3+} couple equilibrates with the $\bullet OOH/O_2$ couple, while Fe^{2+} reduces •OOH to give H_2O_2 (Buettner, 1993; Halliwell and

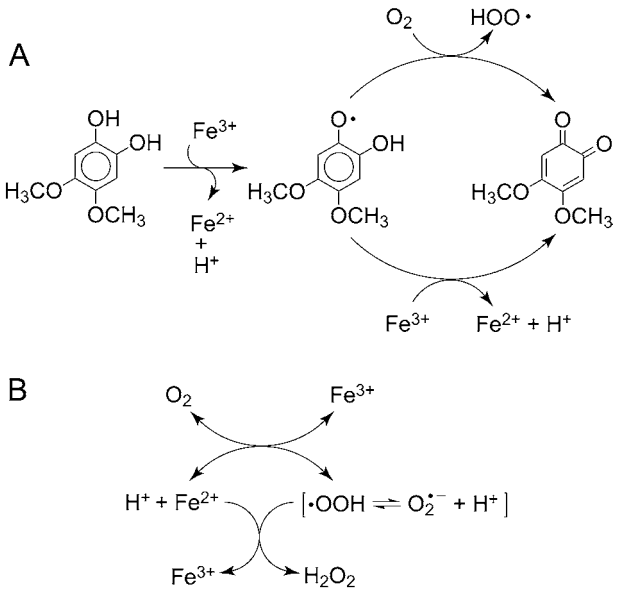

Fig. 1. Reactions of *G. trabeum* hydroquinones that generate Fe^{2+} and H_2O_2, shown here for 4,5-DMC.
A. Reactions of 4,5-DMC and its semiquinone.
B. Subsequent reactions of iron and oxygen species.

Gutteridge, 1999) (Fig. 1). These reactions result in a hydroquinone-driven Fenton system with the following stoichiometry: $3H_2Q + 2O_2 \rightarrow 3Q + 2H_2O + 2{\cdot}OH$ (where H_2Q indicates a hydroquinone and Q the quinone derived from it). In essence, this extracellular biodegradative system exploits the well-documented tendency of hydroquinones to autooxidize in the presence of transition metal ions (Halliwell and Gutteridge, 1999).

Despite the discovery of this mechanism, it has been difficult to assess the importance of hydroquinone-driven Fenton chemistry when *G. trabeum* degrades its natural substrate. One problem is that the requisite, highly labile hydroquinones have not yet been observed in decaying wood. Even if they are present, a larger question is whether the hydroquinones generate enough ·OH to account for a significant fraction of the holocellulose scissions that occur during early decay. Fungi produce a vast array of secondary metabolites (Turner, 1971/1983), and the mere presence of a compound with interesting properties could be of trivial importance if the resulting chemistry is quantitatively insignificant. Given the inhomogeneous structure of wood, an exact assay of hydroquinone-dependent ·OH production in it is probably impossible. However, the general magnitude of this process is obtainable if we can estimate the average steady-state concentrations of the dissolved hydroquinones in decaying wood and the rate constants for their reactions with Fe^{3+} in this environment. Using this approach, we show here that the extracellular hydroquinones produced by *G. trabeum* contribute to brown rot.

Results and discussion

Evidence for decay

When *G. trabeum* was grown on small blocks of spruce, two signs of incipient biodegradation appeared by week one before significant weight loss occurred in the wood. First, the tangential stiffness of the blocks decreased. This measurement chiefly reflects disruption of the hemicellulose because it is taken at right angles to the fibres (Bergander and Salmen, 2002). Second, there was a significant drop in the viscometric degree of polymerization (DP_v) of the holocellulose isolated from the blocks. As viscosity is most affected by scissions of the longest polymers in a mixture, and cellulose chains are much longer than hemicellulose chains, large changes in this measurement indicate depolymerization of the cellulose (Hiemenz, 1984) (Table 1). These results indicated that both components of the holocellulose were attacked at the outset of decay, and suggested that the number of holocellulose scissions might be used to track the number of oxidative events that had occurred in the wood.

By week three, significant weight loss had occurred and was accompanied by a progressive decrease in sample stiffness, as expected when material is removed from the wood (Table 1) (Curling *et al.*, 2002). The holocellulose DP_v did not change significantly after week one, which

Table 1. Properties of spruce wood colonized by *G. trabeum*.

		Stiffness loss[b] (%)		
Week	Weight loss[a] (%)	Inoculated	Control	Holocellulose DP_v[c]
0	ND	ND	0	1280 ± 30
1	–0.4/0.6/1.5	11 ± 2	0 ± 4	640 ± 30
3	4.0/6.8/11.6	47 ± 5	5 ± 4	500 ± 110
5	7.6/14.3/23.5	74 ± 4	7 ± 4	500 ± 170
16	12.7/23.4/50.8	ND	ND	ND

a. 25%/Median/75% quartile analyses with $n = 10$ (week 1), 13 (week 3), 7 (week 5) and 31 (week 16).
b. Averages ± 90% confidence intervals with $n = 5$ (week 1), 4 (week 3) and 5 (week 5).
c. Averages ± 90% confidence intervals with $n = 6$ (week 0), 12 (week 1), 7 (week 3) and 7 (week 5).
ND, not determined.

suggests that at this point the fungus was removing the products of polysaccharide scission as rapidly as it formed them. It was evident from these results that attempts to enumerate the scissions caused by *G. trabeum* in holocellulose must be performed at week one, because it would be impossible to ascertain how many had occurred in the biomass already removed.

Fungal hydroquinones in the wood

To determine whether 2,5-DMHQ and 4,5-DMC were present in the colonized wood, we acetylated entire blocks at week one, thus trapping *in situ* all compounds that carried hydroxyl groups. The fraction extractable from the wood with ethyl acetate was then analysed by gas chromatography/mass spectrometry (GC/MS). The chromatograms of extracts from colonized blocks exhibited two prominent peaks with retention times and mass spectra that matched those of the authentic derivatized hydroquinones, 1,4-diacetoxy-2,5-dimethoxybenzene and 1,2-diacetoxy-4,5-dimethoxybenzene (m/z 254 [M^+], 212 [$M^+ - H_2C{=}C{=}O$], 170 [$M^+ - 2H_2C{=}C{=}O$]). The diacetoxybenzenes were not detected in uninoculated wood (data not shown).

To quantify 2,5-DMHQ and 4,5-DMC in the aqueous phase of decaying wood, we crushed the blocks rapidly and immediately analysed each of the resulting liquid fractions (referred to henceforth as squeezates) by reverse-phase high-performance liquid chromatography (HPLC). As the two hydroquinones coeluted, their concentrations were obtained by taking the differences in concentrations of the two quinones, 2,5-DMBQ and 4,5-DMBQ, before and after the addition of $FeCl_3$ to each sample (Fig. 2). The Fe^{3+} salt was added because it ensured rapid and complete conversion to the quinones by accelerating the rate of hydroquinone autooxidation (Jensen *et al*., 2001). The HPLC analyses showed that 2,5-DMHQ and 4,5-DMC were present from week one in the aqueous phase of all colonized wood blocks and persisted for at least 5 weeks (Table 2).

Iron in the wood

In preliminary work, we found that desferrioxamine inhibited the rate of 2,5-DMHQ autooxidation in squeezates by about 80%, which suggested that Fe^{3+} was the primary oxidant of hydroquinones in the colonized wood (Halliwell and Gutteridge, 1999). We determined the amount of soluble iron in the squeezates by inductively coupled plasma atomic emission spectrometry (ICPAES) and found that the concentration was relatively constant, averaging 11.4 $\pm$ 0.9 μM over the 5 week experiment (Table 2). Most of this iron was Fe^{3+}, because Fe^{2+} was undetectable by the spectrophotometric ferrozine assay.

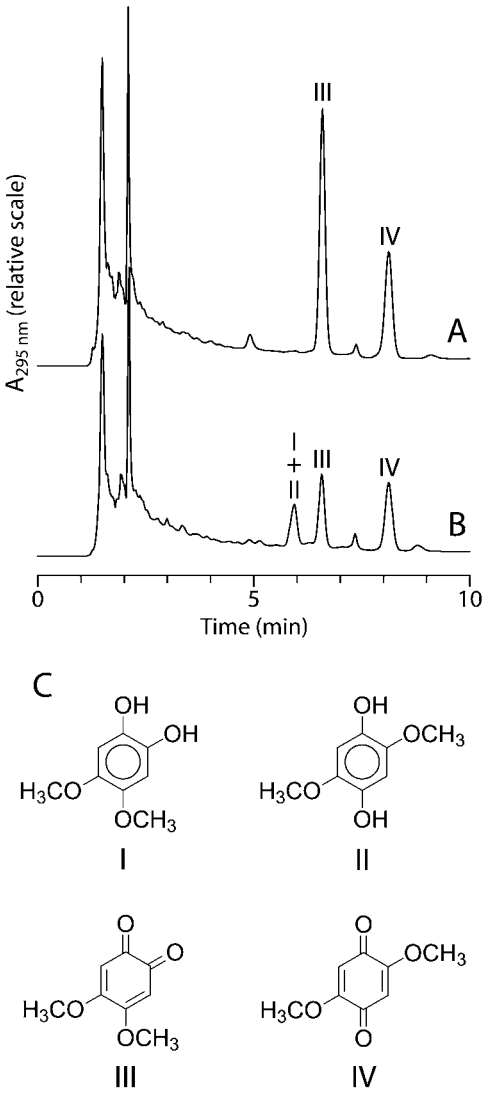

Fig. 2. HPLC analyses of a typical week one squeezate.
A. Products found after oxidation of the sample with Fe^{3+}.
B. Products found when the sample was analysed immediately after crushing the wood block.
C. Structures of products I–IV.

Because the limit of detection for our ferrozine method was about 0.7 μM, the minimum average Fe^{3+} concentration in the aqueous phase of the wood was taken to be 10.7 $\pm$ 0.9 μM. Copper was not detectable in squeezates until week five, when it was 2.6 μM. Therefore, although copper ions can catalyse Fenton chemistry (Halliwell and Gutteridge, 1999), their contribution to decay during week one was undoubtedly small in our experiments.

Rate constants for reactions between hydroquinones and Fe^{3+}

To estimate the rate constants (*k*), it is necessary to make an assumption about how the Fe^{3+} in decaying wood is

Table 2. Concentrations of analytes in squeezates from spruce wood colonized by *G. trabeum*.

	Analyte concentration (μM)				
Week	2,5-DMHQ[a]	4,5-DMC[a]	Iron[b]	Oxalate[c]	pH[b]
1	20.7 ± 5.8	18.9 ± 12.1	11.3	520 ± 80	4.7
3	9.1 ± 2.9	5.9 ± 3.7	12.4	760 ± 340	4.4
5	3.2 ± 0.6	3.8 ± 2.0	10.5	1120 ± 300	4.3

a. Averages ± 90% confidence intervals with $n = 12$ (week 1), 3 (week 3) and 3 (week 5).
b. Squeezates from three blocks pooled for one analysis.
c. Averages ± 90% confidence intervals with $n = 4$ (week 1), 3 (week 3) and 3 (week 5).

complexed, because the redox potentials of different Fe^{3+} chelates vary widely (Buettner, 1993; Halliwell and Gutteridge, 1999). We assumed that oxalate is the predominant chelator in wood undergoing brown rot by *G. trabeum*, because it is the major organic acid secreted by brown rot fungi and because it binds Fe^{3+} much more tightly than do polysaccharides, lignin, or most other organic acids (Espejo and Agosin, 1991; Smith *et al.*, 1998; Varela and Tien, 2003). The oxalate concentration ranged from 520 to 1120 μM, and the pH from 4.3 to 4.7, in squeezates from decaying wood (Table 2). Therefore, a sodium oxalate buffer near the middle of these ranges (750 μM, pH 4.5) was used to determine values of *k*. It was not feasible to determine the rate constants in the squeezates themselves, because they already contained 2,5-DMBQ, 4,5-DMBQ, Fe^{3+} and unidentified coloured compounds that would have interfered with the measurements.

We determined k_{DMHQ} for the reaction between 2,5-DMHQ and Fe^{3+} in sodium oxalate by obtaining time-courses of spectrophotometric data for reactions that started with approximately physiological concentrations of these reactants (Fig. 3A). We assumed that the resulting UV absorption spectra were varying sums of the 2,5-DMHQ, 2,5-DMBQ, Fe^{3+}-oxalate and Fe^{2+}-oxalate absorption spectra. Deconvolution of the experimental spectra into these four contributions yielded time-courses of 2,5-DMHQ disappearance and 2,5-DMBQ appearance. These time-courses fit a simple kinetic model in which the reaction between 2,5-DMHQ and Fe^{3+} is first order in both reactants (Fig. 3B). That is, $d[2,5\text{-DMBQ}]/dt = k_{DMHQ}[2,5\text{-DMHQ}][Fe^{3+}]$. When [2,5-DMHQ] and $[Fe^{3+}]$ are both 10 μM, i.e. near their physiological concentrations, the value of k_{DMHQ} given by this model is 43 ± 6 l mol^{-1} s^{-1}.

To estimate k_{DMC} for the reaction between 4,5-DMC and Fe^{3+}, we first determined the relative initial rates at which 4,5-DMC and 2,5-DMHQ produced Fe^{2+} from Fe^{3+} in sodium oxalate buffer under anoxic conditions. Typical data for this experiment can be seen in a previous report (Jensen *et al.*, 2001). The results showed that, at equimolar hydroquinone concentrations, 4,5-DMC-dependent reduction was 1.5 ± 0.1 times faster than 2,5-DMHQ-

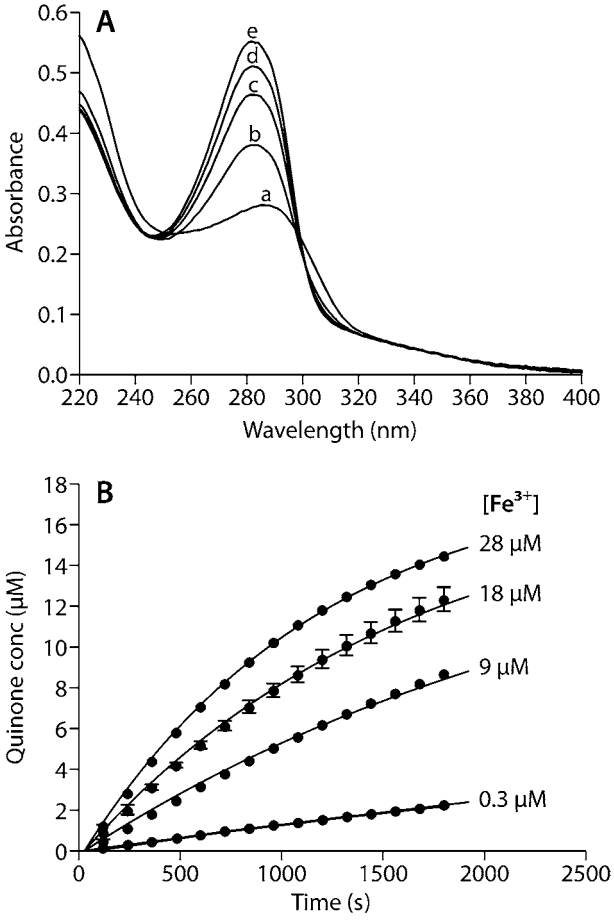

Fig. 3. A. UV/visible absorption spectra obtained in a reaction between 2,5-DMHQ (30 μM) and Fe^{3+} (18 μM) in 750 μM sodium oxalate, pH 4.5. The reaction times shown are (a) 0 s, (b) 600 s, (c) 1200 s, (d) 1800 s and (e) 3600 s.
B. Time-courses of 2,5-DMBQ production in reactions that contained 20 μM 2,5-DMHQ and the indicated concentrations of Fe^{3+} in 750 μM sodium oxalate, pH 4.5. The lines show time-courses predicted by the kinetic model, and the points show values determined from the spectrophotometric data. The spectrophotometric experiment with 18 μM Fe^{3+} was performed three times, and means ± 90% confidence intervals are shown for those results.

dependent reduction (data not shown). As hydroquinones are generally less reducing than their analogous semiquinones (Buettner, 1993; Halliwell and Gutteridge, 1999), we can assume that the initial oxidation of each hydroquinone to its semiquinone by Fe^{3+} is rate-limiting, and therefore the reaction rate ratio of 1.5 equals k_{DMC}/k_{DMHQ}. Given the value of k_{DMHQ} calculated from the spectrophotometric experiments described earlier, and assuming that the reaction between 4,5-DMC and Fe^{3+} is also first order, k_{DMC} is 65 $\pm$ 10 l mol^{-1} s^{-1}.

Estimated contribution of hydroquinone-driven •OH production to holocellulose oxidation

We designed a computer simulation to determine the relationship between the number of oxidative events and the molecular weight distribution of the holocellulose in each decaying wood sample. The simulation assumed that random hits by •OH occurred on cellulose, hemicellulose and lignin in proportion to the fraction of total water that contacted each type of polymer. It also assumed that •OH oxidized the carbon atoms in holocellulose randomly, and that half of these oxidations resulted in chain scission (see *Experimental procedures*). The simulated oxidations generated a series of model cellulose and hemicellulose populations with progressively decreasing DP_v values.

Using this model, we extracted the number of oxidations required to account for the holocellulose depolymerization that we found by viscometry in 12 colonized blocks at week one (Table 1). The calculated values for each sample ($Events_{VISC}$) are plotted on the *y*-axis of Fig. 4. We then used k_{DMHQ} and k_{DMC}, together with the concentrations of hydroquinones and Fe^{3+} in squeezates (Table 2) to estimate the quantity of •OH produced via hydroquinone turnovers in each of the 12 blocks during week one. The values for this quantity ($Events_{HQ}$) are plotted on the *x*-axis of Fig. 4. If hydroquinone-driven Fenton chemistry contributes significantly to wood decay by *G. trabeum*, $Events_{HQ}$ must have the same order of magnitude as $Events_{VISC}$. A cursory inspection of the data shows this to be the case: the mean values for $Events_{HQ}$ and $Events_{VISC}$ are 11.5 and 41.2 μmol events per gram of dry weight of wood respectively. That is, the quantity of •OH expected from hydroquinone turnovers accounts for on average 28% of the holocellulose depolymerization that occurred.

Additional information on the hydroquinone-dependent contribution is obtainable from the plot of $Events_{VISC}$ versus $Events_{HQ}$ (Fig. 4). The diagonal line in this figure represents a linear regression estimate that assumes the variances in the two determinations are equal (Tan and Iglewicz, 1999). Given the assumptions made in developing the model, one would expect the slope of the line to be

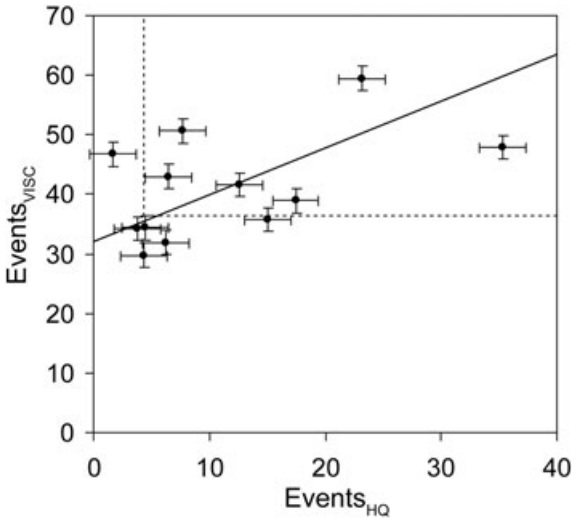

Fig. 4. Plot of $Events_{VISC}$ versus $Events_{HQ}$, both in units of μmol oxidations per gram dry weight of wood. The error bars show 90% confidence intervals estimated from the variability in the data. Points above and to the right of the dashed lines represent samples in which the confidence is $\geq$ 90% that the fungal hydroquinones contributed to holocellulose depolymerization.

1.00. The actual slope of 0.79, with a 90% confidence interval of 0.29–1.73, is in reasonable agreement and lends support to the model's underlying assumptions. The significance test of the hypothesis that this slope is greater than zero gives a *P*-value of 0.029, i.e. there is a 97.1% likelihood that there is a positive correlation between $Events_{HQ}$ and $Events_{VISC}$.

The plot in Fig. 4 also allows an estimate of the number of samples for which we can be 90% confident that hydroquinone-driven oxidations contributed to holocellulose depolymerization. If one subtracts the hydroquinone contribution that the regression line predicts, the contribution of all other mechanisms remains. The average of these values for all 12 samples, which is also the *y*-intercept of the linear regression, is 32.2 μmole events g^{-1}. Assuming that the regression slope is fixed at 0.79, the 90% confidence upper limit of this average hydroquinone-independent contribution is 36.5 μmole events g^{-1}. Furthermore, as our model assumes that the variance in the hydroquinone-independent contribution is the same as the variance in $Events_{HQ}$, the difference between the mean and upper confidence limit for the hydroquinone-independent contribution, 4.3 μmole g^{-1}, corresponds to the minimum value for $Events_{HQ}$ that is different from zero with 90% confidence. When these limits are applied, as indicated by the dashed lines in Fig. 4, it is evident that the hydroquinones played a statistically significant role in six of the 12 samples. For the other six samples no conclusion can be made with 90% confidence about the importance of the hydroquinone-dependent mechanism.

Conclusions

We have calculated that the average amount of hydroquinone-driven •OH production ($Events_{HQ}$) and the average number of oxidations required to account for holocellulose depolymerization ($Events_{VISC}$) had generally similar values in wood undergoing early decay by *G. trabeum*. Our estimates undoubtedly incorporate errors that stem from the assumptions that we had to make regarding the chelation environment for Fe^{3+}, the distribution of water, the efficiency of polysaccharide cleavage by •OH, and other factors. However, the assumptions are based on generally accepted data, and it is unlikely that the errors are so large as to change either of the calculated numbers by an order of magnitude. The significant correlation between $Events_{HQ}$ and $Events_{VISC}$, although not in itself an indication of causality, also supports a hydroquinone-dependent contribution. Therefore, we conclude that the hydroquinones secreted by *G. trabeum* have a role in incipient wood biodegradation.

On the other hand, the existence of a significant *y*-intercept in Fig. 4 shows that there are hydroquinone-independent mechanisms for holocellulose cleavage during early decay. Small Fe^{3+}-reducing peptides or Fe^{3+}-reducing enzymes such as cellobiose dehydrogenase have been proposed to enable extracellular •OH generation by brown rot fungi, and might have been responsible for this result (Enoki *et al*., 1992; Hyde and Wood, 1997). Whatever the nature of the other mechanisms, they may be able to initiate brown rot without a contribution from the hydroquinone-driven system, and it is evident from the data that the various mechanisms are not always expressed coordinately.

Experimental procedures

Reagents

2,5-Dimethoxyhydroquinone, 4,5-dimethoxy-1,2-benzoquinone and 4,5-dimethoxycatechol were prepared as described earlier (Kerem *et al*., 1999; Jensen *et al*., 2001). 2,5-Diacetoxy-1,4-dimethoxybenzene and 4,5-diacetoxy-1,2-dimethoxybenzene were prepared from 2,5-dimethoxy-1,4-benzoquinone and 4,5-dimethoxy-1,2-benzoquinone, respectively, by reductive acetylation with zinc in acetic anhydride (Furniss *et al*., 1989). All other chemicals were reagent grade products from Sigma/Aldrich, except for 2,5-dimethoxybenzoquinone (TCI America) and cupriethylenediamine solution (GFS Chemicals).

Culture conditions

Blocks of spruce wood (*Picea glauca*, $3 \times 10 \times 30$ mm, 302 ± 12 mg dry weight) were cut with the large face perpendicular to the grain. Their dry weights were measured after 24 h at 104°C, after which they were autoclaved twice. For standard cultures, i.e. all except those intended for stiffness analysis, the blocks were then dried under vacuum (approximately 10 mm Hg) for 2 h and infused with 0.3 ml each of sterile 20% potato dextrose broth. Each block was placed on sterile polypropylene mesh over 25 ml of medium containing 1.5% agar in a 250 ml Erlenmeyer flask. The medium, containing mineral salts and a nitrogen source, was made as described earlier (Jensen *et al*., 2001), except that the carbon source (glucose) was omitted. The cultures were inoculated by placing a plug containing actively growing mycelium from a potato dextrose agar plate of *G. trabeum* (ATCC 11539) atop each wood block. Inoculated and uninoculated blocks were then incubated for 1, 3, 5, or 16 weeks at 31°C and 60% relative humidity.

Tangential stiffness of wood

The stiffness of wood blocks was measured both before and after colonization by *G. trabeum*. The blocks were first oven-dried, weighed, autoclaved and saturated with sterile water by vacuum infiltration followed by a 24 h soak. Their stiffness was measured perpendicular to the wood fibres with a Rheometrics DMTA V dynamic mechanical analyser (TA instruments, New Castle, DE). Aseptic conditions were maintained throughout the experiment, and the measurements were made in triplicate at 1 Hz in dual cantilever geometry with a 28 mm span and 0.3% strain. The blocks were removed from the clamp between replicates.

After these initial measurements, the blocks were laid flat on sterile polyethylene mesh and centrifuged for 20 min at 4500 *g* and ambient temperature to remove excess water. Each block was then infused with 0.080 ml of sterile 75% potato dextrose broth to bring it to the same moisture and nutrient levels as in blocks set up by the standard procedure. Cultures were then set up, inoculated and incubated as described in the previous section. At intervals of 1, 3 and 5 weeks, blocks were harvested, dipped in water, and tested again for stiffness. The average stiffness of each block before and after incubation was compared to calculate its per cent decrease in stiffness.

Viscometric analyses of wood holocellulose

Harvested wood blocks were finely diced with a razor blade and delignified with acid chlorite for 6 h at 70°C as described elsewhere (Ahlgren and Goring, 1972). The resulting holocellulose samples were then cooled to room temperature and washed several times with distilled, deionized water (ddH_2O), which was removed by filtration through 0.45 μm pore size nylon filters. The washed samples were dried in a vacuum oven at 50°C and then ground in a Wiley mill to pass a size 20 mesh.

The DP_v values of the milled holocellulose samples were determined as described (TAPPI, 1992) by dissolving them in 0.5% cupriethylenediamine solution and determining their viscosities in Cannon–Fenske capillary viscometer tubes (Cannon Instruments). DP_v values were calculated based on the calibration described earlier (Sihtola *et al*., 1963).

Estimation of the number of oxidations in wood holocellulose

Computer simulations of holocellulose cleavage were implemented in Visual Basic for Microsoft Excel (the computer code and spreadsheet are available from the authors). A model wood composite containing 250 000 holocellulose chains was developed with the following properties: It was assumed to contain (by weight) 39.8% cellulose, 28.6% hemicellulose and 31.6% lignin plus extractives (Sjöström, 1993). Its cellulose was assigned a number-average degree of polymerization (DP_n) of 12 000 and was assumed to be monodisperse (Marx-Figini, 1982). Its hemicellulose was assigned a DP_n of 100 and a polydispersity of 1.22 (Jacobs and Dahlman, 2001). The resulting model composite had a DP_v of 6700.

The molecules in the composite were subjected to a series of random simulated oxidations by •OH. As Fenton chemistry probably occurs in the aqueous phase, the number of oxidations was apportioned among the wood polymers according to their specific water absorptivities (Christensen and Kelsey, 1958; Berry and Roderick, 2005). The apportionment is approximate, because the distribution of water between cellulose, hemicellulose and lignin in wood cannot be obtained on the intact sample, but rather must be determined by comparing isolated fractions of each polymer. This calculation placed 37.0% of the oxidations in cellulose, 44.2% in hemicellulose and 18.8% in lignin plus extractives. Radical attacks on lignin and extractives were counted but assumed not to result in any modification of the holocellulose.

The modelled oxidations of holocellulose by •OH were assumed to occur via random hydrogen abstractions from the anhydrosugar carbons, and 50% of these abstractions were assumed to result in holocellulose cleavage. This cleavage frequency was calculated based on the stoichiometries of published reaction pathways: (i) each oxidation at C1 is assumed to result in polymer scission and the production of one reducing equivalent such as •OOH or Fe^{2+} (Schuchmann *et al*., 1990); (ii) each oxidation at C2, C3, or C6 is assumed to result in the production of one reducing equivalent without polymer scission (von Sonntag *et al*., 1997); (iii) each oxidation at C4 or C5 is assumed to yield a peroxyl radical that consumes two reducing equivalents to become an alkoxyl radical. Each alkoxyl radical then undergoes β-scission to give a hemiacetal ester, which hydrolyses with polymer scission (von Sonntag *et al*., 1997; Isaksson *et al*., 2004). Our assumption that •OH abstracts hydrogens from sugars randomly is approximate, but is supported by published electron spin resonance studies, which showed that these reactions occur with very little regioselectivity (Gilbert *et al*., 1981).

Given the above assumptions, our computer program generated populations of polymer molecules with chain lengths that decreased as a result of the random scissions. By counting the number of molecules with each chain length, the program directly calculated the DP_n value for the composite at each number of oxidative scissions. From that same series of molecular weight distributions, the corresponding holocellulose DP_v values were then calculated by using the standard formula (Hiemenz, 1984) and a Mark–Houwink parameter of 0.9, the value generally accepted for holocellulose (Zhou *et al*., 2004). This tabulation of DP_v values was used to estimate the number of oxidations needed to reduce the DP_v of spruce holocellulose from its initial theoretical value, 6700, to the experimental values we obtained for holocellulose from control and brown-rotted wood. For all samples, this number of oxidations was then corrected for the damage that occurs during the holocellulose isolation and molecular weight determination (Marx-Figini, 1982; Zhou *et al*., 2004). To make the correction, the number of oxidations calculated for each sample was reduced by the number required to reduce the DP_v value of sound spruce holocellulose from its theoretical value of 6700 to its experimental value of 1280. We have reported the corrected numbers as $Events_{VISC}$.

Identification of 2,5-DMHQ and 4,5-DMC in wood

Wood blocks colonized for 1 week and uninoculated blocks were each immersed in 11 ml of acetic anhydride/pyridine (1:1), a threefold excess over the amount required to acetylate all hydroxyl groups in the samples. After several weeks, the separate liquors were poured over ice, adjusted slowly to pH 8.0 with solid sodium carbonate, and extracted twice with one volume of ethyl acetate. The combined ethyl acetate phases were washed once with water, twice with 1 N HCl, once again with water, and then dried over a column of Na_2SO_4. The resulting samples were evaporated and re-dissolved in a small volume of ethyl acetate. A portion of each extract was analysed by GC/MS on a Zebron ZB-5 column (30 m long, 0.25 mm i.d., 0.25 μm film thickness) under the following conditions: carrier gas, argon at 1 ml min^{-1}; injector temperature, 180°C; initial column temperature, 40°C; temperature program, 25°C min^{-1}. 2,5-Diacetoxy-1,4-dimethoxybenzene eluted at 8.18 min, and 4,5-diacetoxy-1,2-dimethoxybenzene at 8.23 min.

Quantification of dissolved reactants in wood

Each harvested wood block was sandwiched between the layers of a folded polypropylene sheet, placed in a large vise with the fold at the bottom, and crushed quickly. The squeezate that collected in the fold comprised about 65% of the 0.759 ± 0.034 ml of water originally present. To quantify 2,5-DMHQ and 4,5-DMC, a portion of the squeezate was taken up in a syringe within 3 s after the block was crushed and immediately analysed by reverse-phase HPLC as described earlier (Jensen *et al*., 2001). A portion of the same sample was then treated with $FeCl_3$ to oxidize the two hydroquinones to their respective quinones, after which the HPLC analysis was repeated. The hydroquinone concentrations in the original squeezate were determined by taking the differences in quinone concentrations before and after $FeCl_3$ treatment. Autooxidation of the hydroquinones during the chromatography was negligible, as shown by the absence of peak tailing.

To look for Fe^{2+} in the wood, a portion of squeezate was immediately mixed with one volume of 1 mM ferrozine in 200 mM sodium oxalate, pH 4.0. An equal portion of the same squeezate was then mixed likewise with the same oxalate buffer lacking ferrozine. The difference spectrum

between the two samples was then taken and the absorbance at 562 nm was recorded ($\varepsilon = 27\,900\ l^{-1}\ mol^{-1}\ cm^{-1}$) (Cowart *et al*., 1993).

To determine total dissolved iron, three frozen squeezates from each harvest time were pooled to obtain a volume of about 1.5 ml and analysed by ICPAES in a Jobin Yvon-Ultima instrument. The pH values of squeezates were also determined on these pooled samples.

To determine oxalate in the squeezates, samples were derivatized with 1,2-diaminobenzene and the resulting quinoxaline was analysed by reverse-phase HPLC as described earlier (McWhinney *et al*., 1986; Hammel *et al*., 1994).

Estimated rates of hydroquinone-dependent •OH production

The rate constant for the reaction between 2,5-DMHQ and Fe^{3+} was estimated by UV/visible absorbance spectrophotometry. Stock solutions of reagents were made daily, using ddH_2O and acid-washed glassware. The solutions were stored in the dark, and in the case of 2,5-DMHQ were also saturated with argon.

The reactions contained sodium oxalate (750 μM, final pH 4.5), $FeCl_3$ (nominally 0, 10, 20, or 30 μM), 2,5-DMHQ (nominally 10, 20, or 30 μM) and α-methyl glucoside (10 mM). The glucoside, which absorbs light negligibly at the wavelengths analysed, was included as a radical trap to minimize oxidation of the reagents by •OH. For each determination, 300 μl of a 10× concentrated reaction mixture containing the oxalate, Fe^{3+}, and glucoside was added to an acid-washed quartz cuvette and diluted with the appropriate volume of ddH_2O, after which the reaction was started by adding 2,5-DMHQ stock solution to give a final volume of 3.00 ml. The reactions were stirred and maintained at 30°C. Spectra were acquired in a Shimadzu MultiSpec-1501 diode array spectrophotometer between 200 and 400 nm every 30 s, beginning 2 s after 2,5-DMHQ addition. The lamp shutter on the spectrophotometer was kept closed between acquisitions and the laboratory was kept dark to minimize the oxalate-dependent photoreduction of Fe^{3+}.

Pure component spectra of 2,5-DMHQ, 2,5-DMBQ and Fe^{3+} were obtained directly from diluted stock solutions in 750 μM sodium oxalate, pH 4.5. The pure component spectrum of Fe^{2+} was approximated by recording the spectrum of a freshly prepared solution and correcting it for the autooxidation to Fe^{3+} that occurred. To make the correction, we first determined that a model assuming first order conversion to Fe^{3+} accounted for the observed changes in the Fe^{2+} spectra. We then subtracted the amounts of Fe^{3+} specified by this kinetic model to obtain the spectrum of Fe^{2+} at zero time.

The concentrations of 2,5-DMHQ, 2,5-DMBQ, Fe^{3+} and Fe^{2+} present in each spectral scan were estimated by using Microsoft Excel Solver and a square difference error term to deconvolute the spectrum into a sum of the four reactants' pure component spectra. The resulting fit to the data was good in the wavelength range at which 2,5-DMHQ and 2,5-DMBQ dominate the spectra (240–400 nm), allowing the hydroquinone and quinone concentrations to be estimated unambiguously for the subsequent kinetic analysis. The contribution from the two iron species, which do not dominate the spectra anywhere, appeared to be confounded with low levels of other species, and was therefore not used for the kinetic analysis.

A kinetic model comprised of three reactions was developed:

$$H_2Q + Fe^{3+} \rightarrow HQ\bullet + Fe^{2+} \quad (1)$$

$$HQ\bullet + O_2/Fe^{3+} \rightarrow Q + \bullet OOH/H_2O_2/Fe^{2+} \quad (2)$$

$$Fe^{2+} + \bullet OOH/H_2O_2/O_2 \rightarrow Fe^{3+} \quad (3)$$

Reaction 1 was assumed to be rate-limiting with a rate constant of k_{DMHQ}, and first order in both reactants. Reaction 2 was assumed to be fast relative to reaction 1, so that when the hydroquinone and Fe^{3+} react the apparent product is the quinone rather than the semiquinone. Reaction 3, with a rate constant of k_{Fe}, was assumed to convert Fe^{2+} rapidly back to Fe^{3+} in accordance with previous results, which showed that Fe^{2+} does not accumulate when Fe^{3+} oxidizes 2,5-DMHQ (Jensen *et al*., 2001).

The disappearance of 2,5-DMHQ and appearance of 2,5-DMBQ that occurred during the rate experiments were fit with the kinetic model, using initial Fe^{3+} concentrations that were set at the values found by ICPAES of the reaction mixtures. The rate equations were integrated using Euler's method with a time step of 1 s (Carnahan *et al*., 1969). The model was then verified by comparison with analytical solutions of the limiting first- and second-order rate expressions. Using Microsoft Excel Solver, a single pair of rate constants, k_{DMHQ} and k_{Fe}, was adjusted to give the least squares difference between the model and the data to seven trials with various levels of Fe^{3+} and 2,5-DMHQ. For each of the trials, the initial 2,5-DMHQ concentration was adjusted to give the best fit of the data. The fitted 2,5-DMHQ concentrations were within 13% of the values calculated from the molarity of the hydroquinone stock solution.

To estimate the rate constant for the reaction between 4,5-DMC and Fe^{3+}, the relative rates of Fe^{3+} reduction by 4,5-DMC and 2,5-DMHQ were determined from initial rates of Fe^{2+} production under anoxic conditions as described earlier (Jensen *et al*., 2001). In this case the relevant reactions are:

$$H_2Q + Fe^{3+} \rightarrow HQ\bullet + Fe^{2+} \quad (1)$$

$$HQ\bullet + Fe^{3+} \rightarrow Q + Fe^{2+} \quad (4)$$

Reaction 1, the less energetically favourable of the two (Buettner, 1993; Halliwell and Gutteridge, 1999), was assumed to be rate-limiting with rate constants of k_{DMHQ} and k_{DMC}. It was also assumed to be first order in both reactants. The anoxic rate for 4,5-DMC was divided by the anoxic rate for 2,5-DMHQ and multiplied by k_{DMHQ} to obtain k_{DMC}. We used this approach because the chemical instability of 4,5-DMC made it difficult to prepare a sufficient purified quantity for experiments like those we used to estimate k_{DMHQ}.

The number of hydroquinone-dependent hits on wood polymers during week one ($Events_{HQ}$) was assumed to be the same as the amount of •OH expected from reactions between the hydroquinones and Fe^{3+} during this time, in accordance with the extremely high reactivity of •OH. $Events_{HQ}$ was estimated by summing the contributions from 2,5-DMHQ and 4,5-DMC. Each of these contributions was estimated to be $k[H_2Q][Fe^{3+}] \times 0.5 \times 0.667 \times 0.000759 \times$

604 800, where the factor of 0.5 assumes the hydroquinone concentration increased linearly from zero during week one, the factor of 0.667 gives the number of •OH radicals produced per hydroquinone turnover, 0.000759 is the volume in litres of water in an average block and 604 800 is the length in seconds of the experiment.

Statistical analyses

Statistics for most replicate measurements appeared consistent with a normal distribution and are expressed as means ± 90% confidence intervals. Weight losses in the wood did not appear normally distributed, and are therefore presented as medians with quartile analyses.

Acknowledgements

We thank K. Hirth for the GC/MS analyses and D. Foster for the ICPAES analyses. This work was funded by US Department of Energy Grant DE-FG01-94ER20140 to K.E. Hammel.

References

Ahlgren, P.A., and Goring, D.A.I. (1972) Removal of wood components during chlorite delignification of black spruce. *Can J Chem* **49:** 172–175.

Bergander, A., and Salmen, L. (2002) Cell wall properties and their effects on the mechanical properties of fibers. *J Mat Sci* **37:** 151–156.

Berry, S.L., and Roderick, M.L. (2005) Plant-water relations and the fibre saturation point. *New Phytol* **168:** 25–37.

Buettner, G.R. (1993) The pecking order of free radicals and antioxidants: lipid peroxidation, α-tocopherol, and ascorbate. *Arch Biochem Biophys* **300:** 535–543.

Carnahan, B., Luther, H.A., and Wilkes, J.O. (1969) *Applied Numerical Methods*. New York, NY, USA: John Wiley and Sons.

Christensen, G.N., and Kelsey, K.E. (1958) The sorption of water vapour by the constituents of wood: determination of sorption isotherms. *Austral J Appl Sci* **9:** 265–282.

Cohen, R., Jensen, K.A., Houtman, C.J., and Hammel, K.E. (2002) Significant levels of extracellular reactive oxygen species produced by brown rot basidiomycetes on cellulose. *FEBS Lett* **531:** 483–488.

Cowart, R.E., Singleton, F.L., and Hind, J.S. (1993) A comparison of bathophenanthrolinedisulfonic acid and ferrozine as chelators of iron(II) in reduction reactions. *Anal Biochem* **211:** 151–155.

Cowling, E.B. (1961) Comparative biochemistry of the decay of sweetgum sapwood by white-rot and brown-rot fungi. *USDA Tech Bull* **1258:** 1–79.

Curling, S.F., Clausen, C.A., and Winandy, J.E. (2002) Relationships between mechanical properties, weight loss, and chemical composition of wood during incipient brown-rot decay. *For Prod J* **52:** 34–39.

Enoki, A., Hirano, T., and Tanaka, H. (1992) Extracellular substance from the brown-rot basidiomycete *Gloeophyllum trabeum* that produces and reduces hydrogen peroxide. *Mater Org* **27:** 247–261.

Espejo, E., and Agosin, E. (1991) Production and degradation of oxalic acid by brown rot fungi. *Appl Environ Microbiol* **57:** 1980–1986.

Flournoy, D.S., Kirk, T.K., and Highley, T.L. (1991) Wood decay by brown-rot fungi: changes in pore structure and cell wall volume. *Holzforschung* **45:** 383–388.

Furniss, B.S., Hannaford, A.J., Smith, P.W.G., and Tatchell, A.R. (eds) (1989) *Vogel's Textbook of Practical Organic Chemistry*. New York, NY, USA: John Wiley and Sons.

Gilbert, B.C., King, D.M., and Thomas, C.B. (1981) Radical reactions of carbohydrates. 2. An electron-spin resonance study of the oxidation of D-glucose and related compounds with the hydroxyl radical. *J Chem Soc Perkin Trans* **2:** 1186–1199.

Halliwell, B., and Gutteridge, J.M.C. (1999) *Free Radicals in Biology and Medicine*. Oxford, UK: Oxford University Press.

Hammel, K.E., Mozuch, M.D., Jensen, K.A., and Kersten, P.J. (1994) H_2O_2 recycling during oxidation of the arylglycerol-β-aryl ether lignin structure by lignin peroxidase and glyoxal oxidase. *Biochemistry* **33:** 13349–13354.

Hammel, K.E., Kapich, A.N., Jensen, K.A., and Ryan, Z.C. (2002) Reactive oxygen species as agents of wood decay by fungi. *Enzyme Microb Technol* **30:** 446–453.

Hiemenz, P.C. (1984) *Polymer Chemistry*. New York, NY, USA: Marcel Dekker.

Hyde, S.M., and Wood, P. (1997) A mechanism for production of hydroxyl radicals by the brown-rot fungus *Coniophora putanea*: Fe(III) reduction by cellobiose dehydrogenase and Fe(II) oxidation at a distance from the hyphae. *Microbiology* **143:** 259–266.

Illman, B.L., Meinholtz, D.C., and Highley, T.L. (1989) Oxygen free radical detection in wood colonized by the brown-rot fungus, *Postia placenta*. *Biodeterior Res* **2:** 497–509.

Isaksson, D., Lindmark-Henriksson, M., Manoranjan, T., Sjodin, K., and Hogberg, H.E. (2004) Hemiacetals and their esters as side-products in lipase-catalysed transesterifications of vinyl esters with sterically hindered alcohols. *J Mol Catal B* **31:** 31–37.

Jacobs, A., and Dahlman, O. (2001) Characterization of the molar masses of hemicelluloses from wood and pulps employing size exclusion chromatography and matrix-assisted laser desorption ionization time-of-flight mass spectrometry. *Biomacromolecules* **2:** 894–905.

Jensen, K.A., Houtman, C.J., Ryan, Z.C., and Hammel, K.E. (2001) Pathways for extracellular Fenton chemistry in the brown rot basidiomycete *Gloeophyllum trabeum*. *Appl Environ Microbiol* **67:** 2705–2711.

Kerem, Z., Bao, W., and Hammel, K.E. (1998) Rapid polyether cleavage via extracellular one-electron oxidation by a brown-rot basidiomycete. *Proc Natl Acad Sci USA* **95:** 10373–10377.

Kerem, Z., Jensen, K.A., and Hammel, K.E. (1999) Biodegradative mechanism of the brown rot basidiomycete *Gloeophyllum trabeum*: evidence for an extracellular hydroquinone-driven fenton reaction. *FEBS Lett* **446:** 49–54.

Kirk, T.K., Ibach, R., Mozuch, M.D., Conner, A.H., and Highley, T.L. (1991) Characteristics of cotton cellulose

depolymerized by a brown-rot fungus, by acid, or by chemical oxidants. *Holzforschung* **45:** 239–244.

Koenigs, J.W. (1974) Hydrogen peroxide and iron: a proposed system for decomposition of wood by brown-rot basidiomycetes. *Wood Fiber* **6:** 66–79.

Kramer, C., Kreisel, G., Fahr, K., Kassbohrer, J., and Schlosser, D. (2004) Degradation of 2-fluorophenol by the brown-rot fungus *Gloeophyllum striatum*: evidence for the involvement of extracellular Fenton chemistry. *Appl Microbiol Biotechnol* **64:** 387–395.

Lindahl, B.O., Taylor, A.F.S., and Finlay, R.D. (2002) Defining nutritional constraints on carbon cycling in boreal forests – towards a less 'phytocentric' perspective. *Plant Soil* **242:** 123–135.

McFee, W.W., and Stone, E.L. (1966) The persistence of decaying wood in the humus layers of northern forests. *Soil Sci Soc Am Proc* **30:** 513–516.

McWhinney, B.C., Cowley, D.M., and Chalmers, A.H. (1986) Simplified column liquid chromatographic method for measuring urinary oxalate. *J Chromatog* **383:** 137–141.

Marx-Figini, M. (1982) The control of molecular weight and molecular-weight distribution in the biogenesis of cellulose. In *Cellulose and Other Natural Polymer Systems: Biogenesis, Structure, and Degradation*. Brown, R.M. (ed.). New York, NY, USA: Plenum Press, pp. 243–271.

Newcombe, D., Paszczynski, A., Gajewska, W., Kroger, M., Feis, G., and Crawford, R. (2002) Production of small molecular weight catalysts and the mechanism of trinitrotoluene degradation by several *Gloeophyllum* species. *Enzyme Microb Technol* **30:** 506–517.

Paszczynski, A., Crawford, R., Funk, D., and Goodell, B. (1999) *De novo* synthesis of 4,5-dimethoxycatechol and 2,5-dimethoxyhydroquinone by the brown rot fungus *Gloeophyllum trabeum*. *Appl Environ Microbiol* **65:** 674–679.

Schlosser, D., Fahr, K., Karl, W., and Wetzstein, H.G. (2000) Hydroxylated metabolites of 2,4-dichlorophenol imply a Fenton-type reaction in *Gloeophyllum striatum*. *Appl Environ Microbiol* **66:** 2479–2483.

Schuchmann, M.N., Schuchmann, H.P., and von Sonntag, C. (1990) Hydroxyl radical induced oxidation of acetaldehyde dimethyl acetal in oxygenated aqueous solution: rapid $O_2{\bullet}^-$ release from the $CH_3C(OCH_3)O_2{\bullet}$ radical. *J Am Chem Soc* **112:** 403–407.

Schultz, T.P., and Nicholas, D.D. (2002) Development of environmentally-benign wood preservatives based on the combination of organic biocides with antioxidants and metal chelators. *Phytochemistry* **61:** 555–560.

Sihtola, H., Kyrklund, B., Laamanen, L., and Palenius, I. (1963) Comparison and conversion of viscosity and DP values determined by different methods. *Paperi ja Puu* **4a:** 225–232.

Sjöström, E. (1993) *Wood Chemistry: Fundamentals and Applications*, 2nd edn. San Diego, CA, USA: Academic Press.

Smith, R.M., Martell, A.E., and Motekaitis, R.J. (1998) *NIST Critically Selected Stability Constants of Metal Complexes Database.* Gaithersburg, MD, USA: National Institute of Standards and Technology.

von Sonntag, C., Dowideit, P., Fang, X.W., Mertens, R., Pan, X.M., Schuchmann, M.N., and Schuchmann, H.P. (1997) The fate of peroxyl radicals in aqueous solution. *Water Sci Technol* **35:** 9–15.

Tan, C.Y., and Iglewicz, B. (1999) Measurement methods comparisons and linear statistical relationship. *Technometrics* **41:** 192–201.

TAPPI (Technical Association of the Pulp and Paper Industry) (1992) Viscosity of pulp (capillary viscometer method), T230 om-89. In *TAPPI Test Methods 1992–1993.* Atlanta, GA, USA: TAPPI Press.

Turner, W.B. (1971/1983) *Fungal Metabolites*, 2 v. London, UK: Academic Press.

Varela, E., and Tien, M. (2003) Effect of pH and oxalate on hydroquinone-derived hydroxyl radical formation during brown rot wood degradation. *Appl Environ Microbiol* **69:** 6025–6031.

Wetzstein, H.-G., Schmeer, N., and Karl, W. (1997) Degradation of the fluoroquinolone enrofloxacin by the brown rot fungus *Gloeophyllum striatum*: identification of metabolites. *Appl Environ Microbiol* **63:** 4272–4281.

Zhou, J., Zhang, L., and Cai, J. (2004) Behavior of cellulose in NaOH/urea aqueous solution characterized by light scattering and viscometry. *J Polym Sci B* **42:** 347–353.